Resource

Molecular Cell

Lipidomics Analyses Reveal Temporal and Spatial Lipid Organization and Uncover Daily Oscillations in Intracellular Organelles

Graphical Abstract

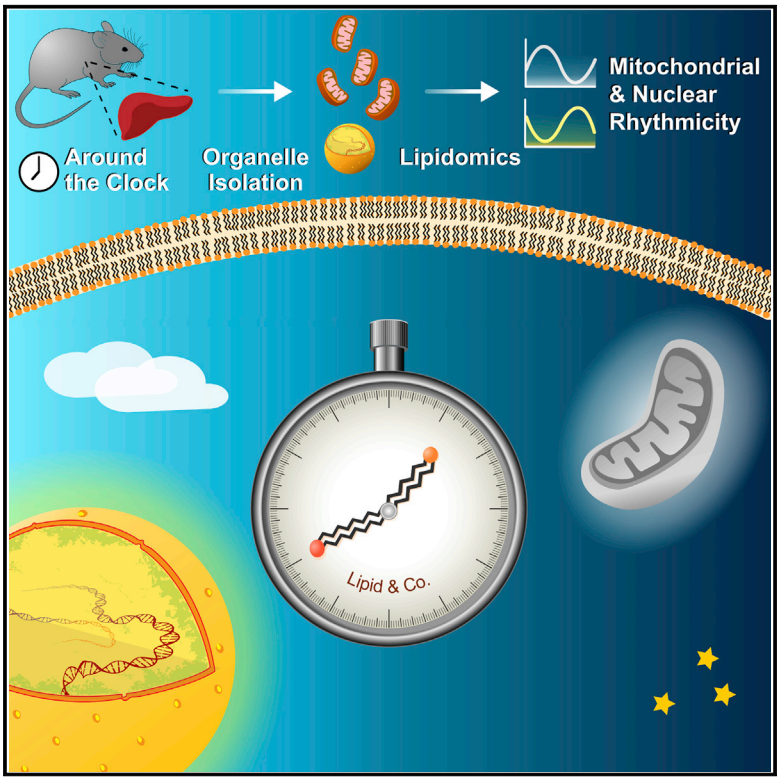

Authors

Rona Aviram, Gal Manella, Naama Kopelman, ..., Chunyan Wang, Xianlin Han, Gad Asher

Correspondence

gad.asher@weizmann.ac.il

In Brief

Aviram et al. performed lipidomics analyses of organelles from mouse liver to explore temporal and spatial principles in lipid organization. They find that the lipid composition of the nucleus and mitochondria oscillates daily with distinct and opposite phases. These oscillations respond to feeding time and are coordinated by the circadian clock.

Highlights

- Temporal and spatial lipidomics analyses reveal principles in lipid organization
- The lipid composition of the nucleus and mitochondria exhibits daily oscillations
- Oscillations in subcellular organelles are anti-phasic and respond to feeding time
- The circadian clock coordinates the phase relation between the two organelles

Aviram et al., 2016, Molecular Cell 62, 636–648
May 19, 2016
http://dx.doi.org/10.1016/j.molcel.2016.04.002

CellPress

CellPress

Molecular Cell
Resource

Lipidomics Analyses Reveal Temporal and Spatial Lipid Organization and Uncover Daily Oscillations in Intracellular Organelles

Rona Aviram,[1] Gal Manella,[1] Naama Kopelman,[2] Adi Neufeld-Cohen,[1] Ziv Zwighaft,[1] Meytar Elimelech,[1] Yaarit Adamovich,[1] Marina Golik,[1] Chunyan Wang,[3] Xianlin Han,[3] and Gad Asher[1,*]
[1]Department of Biomolecular Sciences
[2]Department of Biological Services
Weizmann Institute of Science, 7610001 Rehovot, Israel
[3]Center for Metabolic Origins of Disease, Sanford Burnham Prebys Medical Discovery Institute, Orlando, FL 32827, USA
*Correspondence: gad.asher@weizmann.ac.il
http://dx.doi.org/10.1016/j.molcel.2016.04.002

SUMMARY

Cells have evolved mechanisms to handle incompatible processes through temporal organization by circadian clocks and by spatial compartmentalization within organelles defined by lipid bilayers. Recent advances in lipidomics have led to identification of plentiful lipid species, yet our knowledge regarding their spatiotemporal organization is lagging behind. In this study, we quantitatively characterized the nuclear and mitochondrial lipidome in mouse liver throughout the day, upon different feeding regimens, and in clock-disrupted mice. Our analyses revealed potential connections between lipid species within and between lipid classes. Remarkably, we uncovered diurnal oscillations in lipid accumulation in the nucleus and mitochondria. These oscillations exhibited opposite phases and readily responded to feeding time. Furthermore, we found that the circadian clock coordinates the phase relation between the organelles. In summary, our study provides temporal and spatial depiction of lipid organization and reveals the presence and coordination of diurnal rhythmicity in intracellular organelles.

INTRODUCTION

A fundamental principle in cell biology is the temporal and spatial partitioning of different cellular processes that are chemically incompatible. Organisms have evolved various mechanisms to distribute biological processes to different subcellular structures such as organelles and/or to separate them to distinct time windows. The former is often achieved by generating a physical barrier in the form of a lipid bilayer membrane, whereas the latter is attained, in part, through the temporal coordination of different processes by biological clocks.

All light-sensitive organisms harbor time-measuring devices, known as circadian clocks, which orchestrate their daily physiology. In mammals, a master clock in the brain is entrained by daily light/dark cycles and synchronizes clocks in peripheral organs in part by driving rhythmic feeding behavior. In fact, circadian oscillations are present in almost every cell in the body, and are believed to function based on interlocked transcription-translation feedback loops (Partch et al., 2014). The presence of cell-autonomous oscillations raises the question of whether circadian oscillations are also found in intracellular organelles, a conjecture that thus far has never been thoroughly examined.

Circadian clocks regulate lipid homeostasis, and disruption of circadian rhythmicity is associated with obesity and metabolic syndrome (Adamovich et al., 2015; Bass, 2012; Feng and Lazar, 2012). Lipids participate in a wide variety of cellular processes such as energy storage and signal transduction; however, the bulk of cellular lipids play an essential role in the structure/function of biological membranes of cells and organelles, and hence measurably define their identity (van Meer et al., 2008). Even subtle changes in membrane lipid composition can have a tremendous impact on membrane properties and related functions (Klose et al., 2013). Recent advances in lipidomics approaches have enabled the identification and characterization of hundreds of lipid species (Brügger, 2014; Han et al., 2012; Shevchenko and Simons, 2010). Yet, in comparison to our extensive knowledge on gene expression or protein networks, our understanding of lipid organization is lagging behind. Moreover, lipid analyses have mostly centered on whole cells or tissue samples at a single time point. When such approaches are taken, information regarding the subcellular distribution of different lipids and their temporal dynamics is completely lost.

In this study, we examined the two aforementioned trajectories, namely spatial and temporal organization, and quantified hundreds of lipid species in the nucleus and mitochondria throughout the day. We specifically inspected (1) the lipid composition of the different organelles, (2) the temporal changes in their lipid composition throughout the day, and (3) the effect of feeding and circadian clocks on lipid organization. Interestingly, we uncovered diurnal oscillations in the nucleus and mitochondria with distinct and opposite phases. These oscillations readily responded to feeding time and were coordinated by the circadian clock. Our spatiotemporal analyses provide insights regarding lipid organization in general and concerning the

presence and nature of diurnal rhythmicity in subcellular organelles specifically.

RESULTS

The Nuclear and Mitochondrial Lipidome

We set out to analyze the daily lipid composition of two principal intracellular organelles, namely the nucleus and mitochondria, in mouse liver. To this aim, mice were sacrificed at 4-hr intervals throughout the day, livers were harvested, and nuclei and mitochondria were biochemically fractionated. As expected, SDS-PAGE and immunoblot analysis of the nuclear (nucleus) and mitochondrial (mitochondria) fractions showed that these fractions are highly enriched for nuclear (e.g., U2AF) and mitochondrial (e.g., GLUD1) proteins, respectively (Figure S1A). Because both the nucleus and mitochondria are in close vicinity to other intracellular organelles, we also examined the presence of protein markers for the ER (e.g., BiP), ER-Golgi (e.g., ERGIC-53), plasma membrane (e.g., EGFR), cytoplasm (e.g., TUBULIN), and endosome (e.g., EE1A) (Figure S1A). Although some of these protein markers could be detected in our samples, their levels were low and relatively constant throughout the day.

Next, we applied shotgun lipidomics (Han et al., 2012; Wang et al., 2016) to identify and quantify the lipid constituents of the nucleus and mitochondria. A total of 222 individual lipid species were quantified; these include different glycerophospholipid classes (i.e., cardiolipin [CL], lysocardiolipin [LCL], lysophosphatidylethanolamine [LPE], phosphatidic acid [PA], phosphatidylcholine [PC], phosphatidylethanolamine [PE], phosphatidylglycerol [PG], phosphatidylinositol [PI], and phosphatidylserine [PS]) and sphingolipid classes (i.e., ceramide [CER] and sphingomyelin [SM]) (Figure 1A). Overall, 152 and 217 lipid species were quantified in the nucleus and mitochondria, respectively (Tables S1A and S1B); out of these, 147 were present in both organelles (Figure 1B). Five lipid species, LPE 20:3, PA 18:0-20:4, PE D18:0-18:0, PE P16:0-22:6, and PE P18:2-20:4, were exclusively identified in the nucleus. In mitochondria, 70 lipid species were unique and, as expected, mainly consisted of CL and LCL (Osman et al., 2011; van Meer et al., 2008). In line with previous reports (Andreyev et al., 2010; Bird et al., 2013), a large bulk of lipids in both compartments involved glycerophospholipids, primarily PC, with considerable amounts of PI and PE (Figure 1C). Additionally, the total lipid-to-protein ratio was higher (~4-fold) in mitochondria compared to the nucleus, with a similar trend for each of the different lipid classes (Figure 1D).

To examine the lipid organization within the two organelles, we first inspected the daily changes in the nuclear and mitochondrial lipidome. Overall, the different lipid species in mitochondria exhibited a more diverse temporal behavior compared to the nucleus (median r values of 0.53 and 0.22 of pairwise correlation analysis in the nucleus and mitochondria, respectively) (Figures 2A and S2A). Unexpectedly, within lipid classes, the correlation between the different lipid profiles appeared highly variable, albeit with some exceptions, such as PG and SM in the nucleus and LCL and SM in mitochondria (Figures 2B and S2B).

The lack of coherent behavior within the different lipid classes prompted us to employ an unbiased approach. Thus, we categorized lipids in each compartment based on similarities in their daily accumulation profiles. Our working premise was that lipids that exhibit comparable temporal profiles are likely to be co-regulated or might even function together. Using hierarchical clustering, we defined 8 and 13 distinct lipid clusters in the nucleus and mitochondria, respectively (Figures 2C and 2D; Table S2). These clusters exhibited a wide range of temporal profiles (e.g., single peak, double peaks with diverse phases). A few clusters were enriched for certain lipid families; for example, cluster B in the nucleus was enriched for SM. In mitochondria, cluster H was enriched for CL, and cluster J for PC (Figure 2D). However, in most cases, the lipid composition within the clusters was not enriched for a certain lipid class, suggesting that lipid species from various classes might be co-regulated and/or functionally related.

Hitherto, we characterized the lipid landscape of the different organelles. The temporal organization of the nuclear lipidome appeared to be more homogeneous compared to mitochondria. Remarkably, in both compartments, some lipid species exhibited very similar temporal accumulation profiles independent of their classes.

Diurnal Oscillations in the Nucleus and Mitochondria

Our temporal cluster analysis disclosed that some lipid species, both in the nucleus and mitochondria, exhibit diurnal rhythmicity (i.e., a single peak within a 24-hr cycle). Hence, to specifically uncover diurnal oscillations in subcellular compartments, a widely used nonparametric algorithm, JTK_CYCLE, was applied (Hughes et al., 2010). Out of the 152 lipids in the nucleus and 217 lipids in mitochondria, 51 (34%) and 67 (31%), respectively, were identified as oscillating with p value <0.05 (Figure 3A; Tables S3A and S3B). In both organelles, oscillating lipids exhibited similar median amplitude (~2), and predominantly consisted of PC and PE species. Analysis of the peak accumulation time for the different oscillating lipids revealed that the vast majority of lipid species in the nucleus peaked early in the light phase, at zeitgeber time (ZT) 2–4. By contrast, most cycling lipids in mitochondria reached their zenith levels at the transition from the light to the dark phase, namely between ZT10 and ZT14 (Figure 3B). For example, the majority of PC and SM species accumulated at ZT0–4 in the nucleus, as opposed to ZT12–14 in mitochondria. Furthermore, out of 101 oscillating species, many cycled exclusively in the nucleus or mitochondria, whereas 19 overlapped between both compartments, mainly reaching peak levels in each compartment ~12 hr apart (Figure 3C). It is conceivable that the distinct temporal and spatial accumulation of these overlapping lipid species is associated with their specific functions in the nucleus and mitochondria during different times of the day. Among these 19 lipids, 15 belonged to the PC and SM classes that share a choline head group, including PC18:0-18:1. PC18:0-18:1 is regulated by diurnal hepatic PPARγ activity and controls fatty acid usage (Liu et al., 2013). Thus, PC18:0-18:1 accumulation 12 hr apart in the nucleus and mitochondria might be related to its role in fatty acid homeostasis.

Taken together, our analysis uncovered marked diurnal oscillations in the nucleus and mitochondria, with distinct and opposed (~12 hr) peak times.

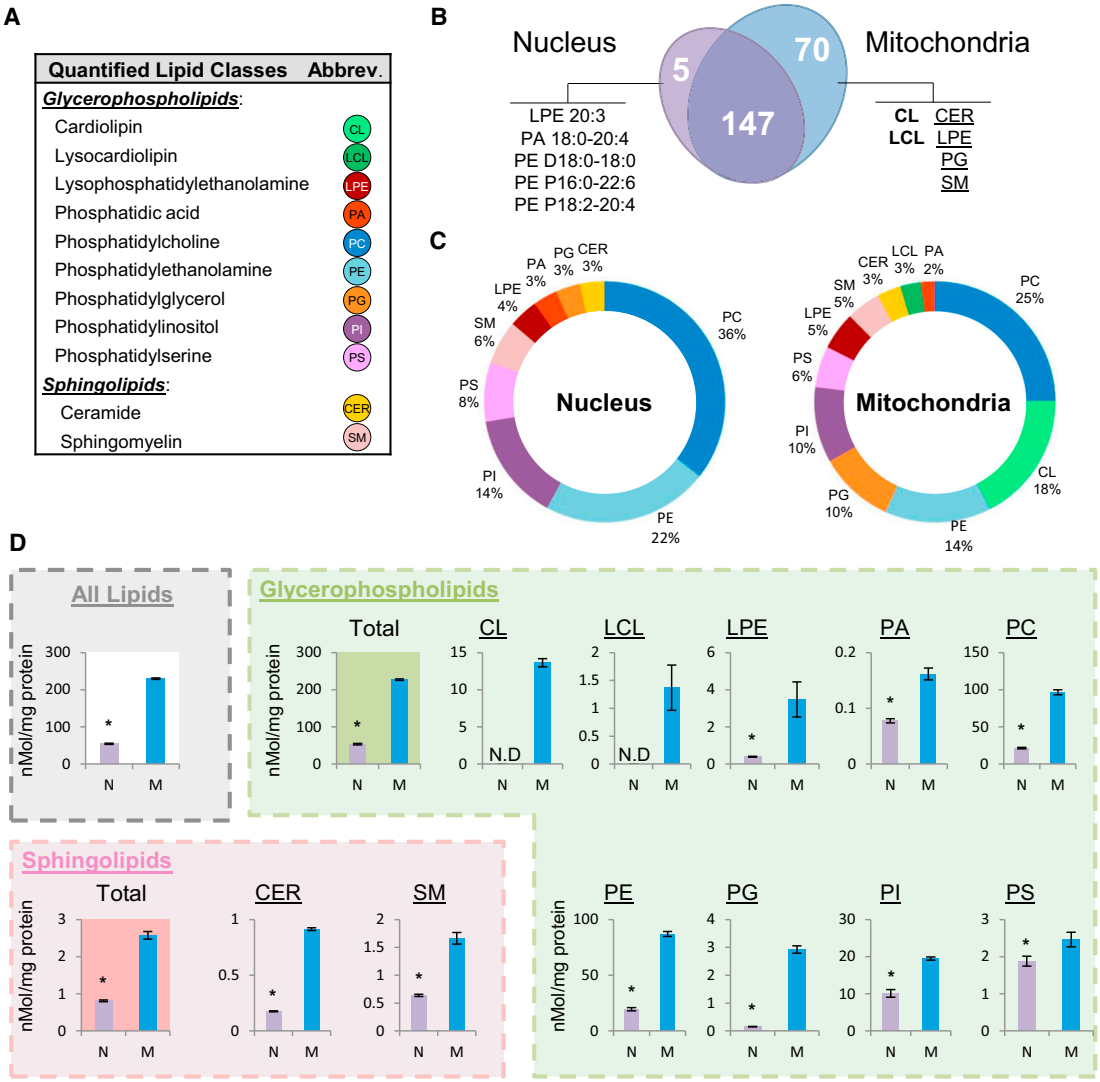

Figure 1. The Nuclear and Mitochondrial Lipidome

(A) Quantified lipid classes, their color code, and abbreviation. The indicated color code and abbreviation are used consistently throughout the paper.

(B) The number of lipid species quantified exclusively in the nucleus (purple), mitochondria (blue), or both organelles. For each compartment the unique lipid species or classes are listed below (bold, complete classes; underlined, partial classes) (for details, see Table S1).

(C) Distribution of the different lipid classes in each organelle.

(D) Comparison between the mean levels of the different lipid classes in the nucleus (N) and mitochondria (M). Data are presented as mean ± SD (six time points, n = 4 for each); *p < 0.005. N.D., nondetected classes.

Feeding Time Regulates the Lipid Composition of the Different Organelles and Their Daily Oscillations

Feeding time serves as a dominant timing cue for clocks in peripheral organs such as the liver (Damiola et al., 2000). Mice normally ingest ~70% of their total food consumption during the dark phase and ~30% during the light phase (Vollmers et al., 2009). Nighttime-restricted feeding was shown to have profound effects on rhythmic gene expression (Vollmers et al., 2009) and on lipid accumulation in whole-liver samples (Adamovich et al., 2014). This prompted us to examine the effect of feeding time on lipid composition and oscillations in intracellular compartments. To this aim, we performed lipidomics analysis of nuclei and mitochondria from livers of mice fed exclusively during the night. The nuclei and mitochondria were highly enriched for nuclear and mitochondrial proteins, respectively, and marker protein levels of other intracellular compartments were low and relatively constant throughout the day (Figure S1B). Intriguingly, merely restricting food availability to nighttime induced remarkable changes in the lipid composition of the different organelles (Figure S3; Tables S4A and S4B), although the total daily food consumption and composition are similar (Adamovich et al., 2014). In the nucleus, we detected ~30% more lipid species in night-fed compared to ad libitum-fed animals (199 and 152 species, respectively) (Figure S3A), whereas in mitochondria a relatively

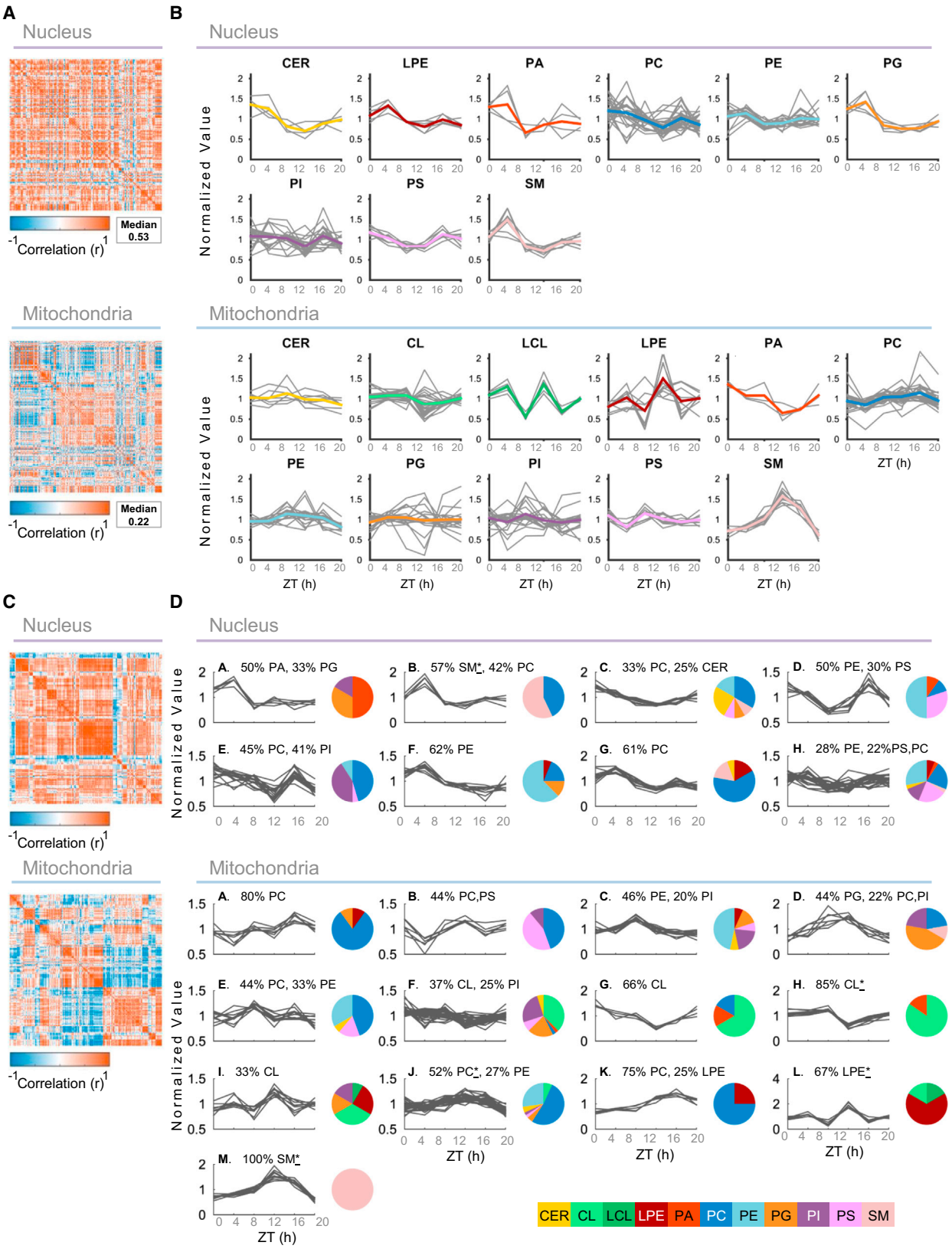

(legend on next page)

similar number of lipid species were identified under both feeding regimens (217 and 227 lipid species in ad libitum- and night-fed animals, respectively) (Figure S3B). These changes are discussed in detail below (see Comparison of the Nuclear and Mitochondrial Lipidome in Wild-Type and Clock-Disrupted Mice under Different Feeding Regimens).

Next, we examined the lipid species that exhibit diurnal oscillations in the different compartments under nighttime-restricted feeding. A JTK_CYCLE-based analysis showed that out of 199 lipid species measured in the nucleus 106 oscillated, and 50 out of 227 oscillated in mitochondria (53% and 22%, respectively) (median amplitude of 2.1 in both compartments) (Figure 4A; Tables S4C and S4D). Thus, nighttime-restricted feeding led to an increase in the fraction of cycling lipids in the nucleus, whereas in mitochondria a moderate decrease was observed (34%–53% in the nucleus and 31%–22% in mitochondria in ad libitum- and night-fed animals, respectively). The oscillating lipid population differed from the one observed for wild-type mice fed ad libitum (Figures S3C and S3D). Intriguingly, even more dramatic changes were detected in the phases of lipid accumulation in each compartment. Under nighttime-restricted feeding, the vast majority of oscillating lipid species accumulated in the nucleus at ~ZT12, whereas in mitochondria they peaked at ~ZT0 (Figure 4B). This is in sharp contrast to the pattern observed for mice fed ad libitum (compare Figures 3B and 4B). Hence, the peak in lipid accumulation was completely inverted to the one observed in mice fed ad libitum, yet the phase relation of ~12 hr between the two organelles prevailed. Specifically, the number of oscillating PC and PE species was increased in the nucleus and peaked at the opposite phase compared to mice fed ad libitum. By contrast, the elevated number of cycling CL species in mitochondria retained their original phase. Here again, the cycling lipid species common to both compartments mainly reached their peak levels ~12 hr apart, whereas others were oscillating exclusively in the nucleus or mitochondria (Figure 4C).

As mentioned above, we identified a number of lipid species that exhibit two peaks throughout the day in wild-type mice fed ad libitum. Remarkably, the majority were nuclear lipids with one peak early in the light phase and a second peak in the middle of the dark phase. Upon nighttime feeding, most of these lipids displayed a single peak at ~ZT12 (Figure S4).

Taken together, we found that nighttime-restricted feeding not only alters the total lipid composition but also imposes reprogramming of oscillations in the different organelles. This includes loss of oscillation of a large number of normally oscillating lipids; dramatic phase changes in an additional subset of oscillating species; and induction of de novo oscillations. However, despite these multiple changes, the general ~12-hr phase relation between the nucleus and mitochondria was retained under both feeding regimens, suggesting that their oscillations are interlocked.

The Lipid Oscillations in the Nucleus and Mitochondria Are Coupled by the Circadian Clock

The above-described analyses uncovered daily oscillations in the nucleus and mitochondria that are responsive to feeding time. Remarkably, the ~12-hr phase relation between the organelles was maintained under different feeding regimens, suggesting that they are coupled to each other. Because circadian clocks play a role in the temporal organization of various biological processes, we examined whether they might coordinate the oscillations in the two organelles. Hence, we performed lipidomics analysis of isolated nuclei and mitochondria prepared from *Per1/2*$^{-/-}$ mice. Mice lacking both PER1 and PER2 exhibit arrhythmic locomotor activity under constant darkness, and circadian expression of core clock and clock-controlled genes is largely diminished (Adamovich et al., 2014; Zheng et al., 2001). In contrast to wild-type mice, clock-disrupted mice such as the *Per1/2*$^{-/-}$ mice consume almost equal amounts of food throughout the day (Adamovich et al., 2014). In order to eliminate the confounding effect of their different eating habits, food availability was therefore restricted to the dark phase. Here again, the nuclei and mitochondria were highly enriched for nuclear and mitochondrial proteins, respectively, and marker protein levels of other intracellular compartments were low and relatively constant throughout the day (Figure S1C). Lipidomics analysis of nuclei and mitochondria prepared from night-fed *Per1/2*$^{-/-}$ mice identified a similar number of lipid species in the two organelles compared to night-fed wild-type mice (Figures S3A and S3B; Tables S5A and S5B).

JTK_CYCLE analysis of isolated nuclei and mitochondria from night-fed PER1/2 null mice showed that in the nucleus 36 out of 200 quantified lipid species were oscillating (~18%) and in mitochondria there were 34 out of 229 (~15%), with median amplitudes of 1.8 and 2, respectively (Figure 5A; Tables S5C and S5D). Thus, the percentage of oscillating lipids in the different organelles dropped compared to night-fed wild-type mice, and this effect was more prominent in the nucleus. Overall, the overlap between the compositions of oscillating lipids in all three tested conditions was low (Figures S3C and S3D).

Figure 2. Temporal Analysis of the Nuclear and Mitochondrial Lipidome

(A) Correlation matrix sorted by lipid class; coloring represents the level of correlation between the lipid pairs. Rows and columns correspond to the 152 and 217 lipid species measured in the nucleus (top) and mitochondria (bottom), respectively. The correlation distribution is presented in Figure S2A.

(B) Daily profiles of the different lipid species, clustered by class, as measured in the nucleus (top) and mitochondria (bottom). Values are normalized to each lipid mean value. The thick colored line in each plot represents the average of the class. Intra-class variability, raw profiles, and amplitude are presented in Figures S2B–S2D, respectively.

(C and D) Hierarchical clustering based on standardized Euclidean distance. (C) Correlation matrix of the lipidome of the nucleus (top) and mitochondria (bottom). (D) Daily profiles of the different lipid species, according to hierarchical clustering. Values are normalized to each lipid mean value. To the right of each plot a pie chart indicates the lipid class distribution within the cluster; the percentage of the prominent classes within the cluster is indicated. Asterisks indicate enriched classes based on FWER <0.025.

See also Table S2.

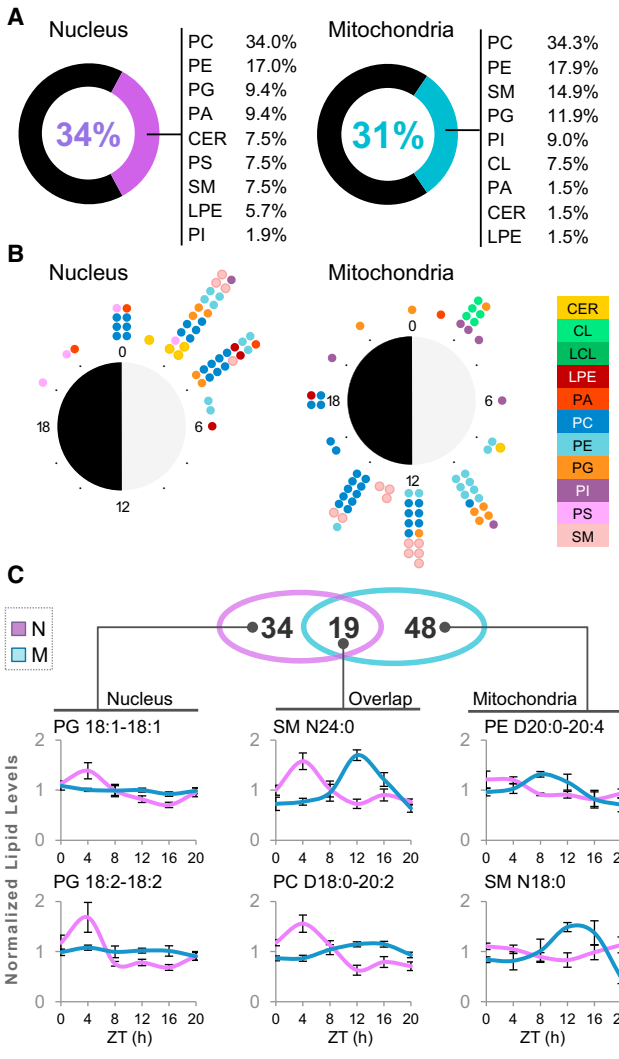

Figure 3. Diurnal Oscillations of Lipid Species in the Nucleus and Mitochondria of Wild-Type Mice Fed Ad Libitum

(A) The percentage of lipid species that exhibit daily oscillations with a single peak in a 24-hr cycle, based on JTK_CYCLE analysis (six time points, n = 4 for each; $p < 0.05$); 51 lipid species out of 152 cycled in the nucleus and 67 out of 217 cycled in the mitochondria (34% and 31%, respectively). Stemming from the pie chart of each organelle is the distribution of cycling lipids based on their lipid classes.

(B) Daytime distribution of the different oscillating lipid species in the nucleus and mitochondria according to their peak phases. Lipids are colored coded by class.

(C) Daily accumulation profiles of representative lipid species, which were found to oscillate either exclusively in the nucleus (left), mitochondria (right), or in both organelles (middle). Data are presented as normalized values ± SEM (n = 4). ZT, zeitgeber time. ZT0 is when the light was turned on, and ZT12 is when the light was turned off.

See also Figure S3 and Table S3.

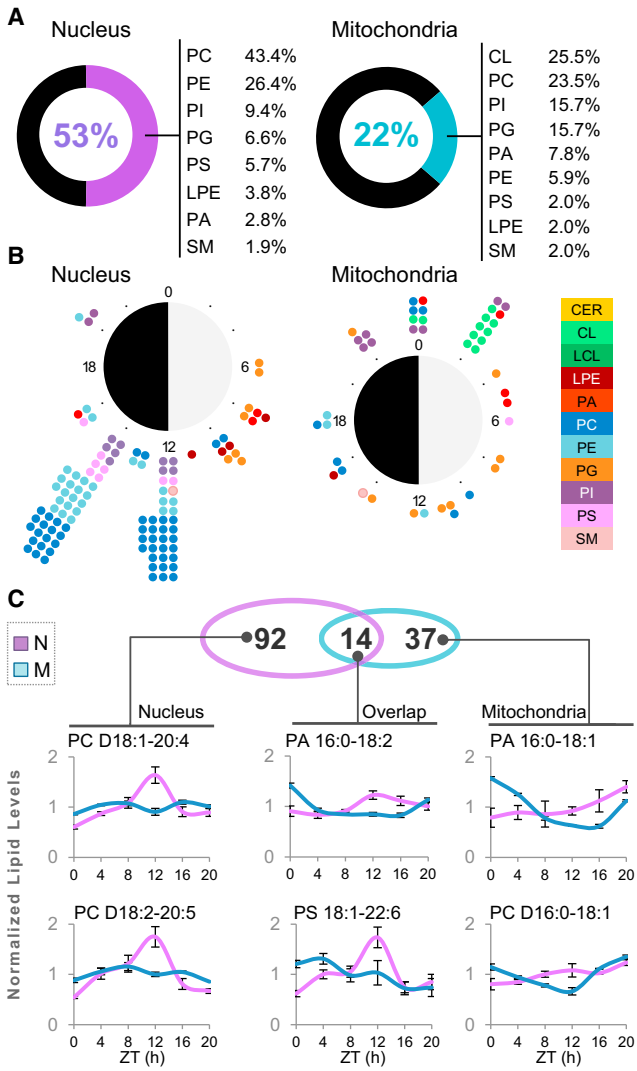

Figure 4. Diurnal Oscillations of Lipid Species in the Nucleus and Mitochondria of Wild-Type Mice Fed Exclusively during the Night

(A) The percentage of lipid species that exhibit daily oscillations with a single peak in a 24-hr cycle, based on JTK_CYCLE analysis (six time points, n = 4 for each; $p < 0.05$); 106 lipid species out of 199 cycled in the nucleus and 50 out of 227 cycled in the mitochondria (53% and 22%, respectively). Stemming from the pie chart of each organelle is the distribution of cycling lipids based on their lipid classes.

(B) Daytime distribution of the different oscillating lipid species in the nucleus and mitochondria according to their peak phases. Lipids are colored coded by class.

(C) Daily accumulation profiles of representative lipid species, which were found to oscillate either exclusively in the nucleus (left), mitochondria (right), or in both organelles (middle). Data are presented as normalized values ± SEM (n = 4).

See also Figure S3 and Table S4.

Strikingly, both in the nucleus and mitochondria, the oscillating lipids exhibited a wide range of peak times, predominantly during the dark phase (Figure 5B). Thus, in the absence of PER1 and PER2, not only was the phase coherence in each of the different organelles derailed but also the ~12-hr phase relation between the nucleus and mitochondria was completely lost. We concluded that PER1/2 and likely the circadian clock couple the lipid oscillations in the nucleus and mitochondria.

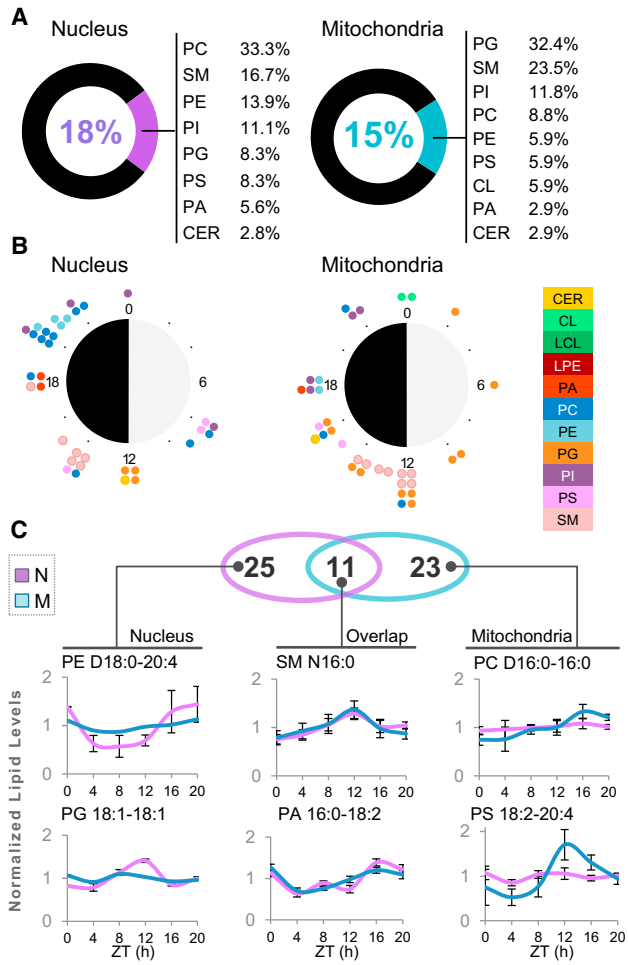

Figure 5. Diurnal Oscillations of Lipid Species in the Nucleus and Mitochondria of *Per1/2*$^{-/-}$ Mice Fed Exclusively during the Night

(A) The percentage of lipid species that exhibit daily oscillations with a single peak in a 24-hr cycle, based on JTK_CYCLE analysis (six time points, n = 4 for each; $p < 0.05$); 36 lipid species out of 200 cycled in the nucleus and 34 out of 229 cycled in the mitochondria (18% and 15%, respectively). Stemming from the pie chart of each organelle is the distribution of cycling lipids based on their lipid classes.

(B) Daytime distribution of the different oscillating lipid species in the nucleus and mitochondria according to their peak phases. Lipids are colored coded by class.

(C) Daily accumulation profiles of representative lipid species, which were found to oscillate either exclusively in the nucleus (left), mitochondria (right), or in both organelles (middle). Data are presented as normalized values ± SEM (n = 4).

See also Figure S3 and Table S5.

Comparison of the Nuclear and Mitochondrial Lipidome in Wild-Type and Clock-Disrupted Mice under Different Feeding Regimens

To dissect the effect of the circadian clock and feeding time on the spatiotemporal changes in lipid accumulation, we performed cross-analysis of our lipidomics data under the different experimental conditions. Notably, the total lipid levels in the nucleus were elevated upon nighttime-restricted feeding (both in wild-type and PER1/2 null mice). By contrast, we did not observe a significant effect of nighttime feeding on total lipid levels in mitochondria (Figure 6A). Comparison of the relative abundance of the different lipid classes further unveiled that certain lipid classes are highly affected by nighttime feeding whereas others are relatively resilient (Figure 6B). Nighttime feeding strongly affected nuclear PE and PI abundance, whereas the relative levels of PC, CER, and PG were unaffected. In mitochondria, PC and PE levels were altered upon nighttime feeding of wild-type mice. This analysis evinced that lipid classes differentially respond to feeding in an organelle-specific manner. We also examined specific properties of the lipids' fatty acid chain, namely length and saturation, regardless of the lipid classes. In both organelles, these two factors were elevated upon nighttime feeding in wild-type and *Per1/2*$^{-/-}$ mice (Figure S5A).

Next, we examined the daily lipid accumulation profiles in the two compartments (Figure 6C). Overall, the total lipid levels exhibited daily oscillations both in the nucleus and mitochondria of wild-type mice fed ad libitum with opposite phases (Figures S5B and S5C). Notably, the prevalence of daily oscillations was higher for some lipid classes (e.g., PG and SM) and the propensity of oscillating lipid classes was elevated in the nucleus compared to mitochondria (Figure 6D). Hence, nighttime feeding both generated de novo oscillations and shifted the phase of existing oscillations in the nucleus of wild-type mice. Additionally, the circadian accumulation of PG and PS in the nucleus was lost in night-fed PER1/2 null mice, suggesting that their oscillations are circadian clock dependent. Interestingly, although PC and PE levels were highly variable throughout the day, in the nucleus and mitochondria, under the different experimental setups (Figure 6C), their ratio was consistently kept constant throughout the day (Figure S5D).

Finally, as described in the above sections, analysis of the different lipid species revealed marked diurnal oscillations in the nucleus and mitochondria, with relatively opposed (~12 hr) peak times that respond to feeding and are coordinated by PER1/2 and likely the circadian clock (Figure 6E).

The Co-regulation of Different Lipid Species in the Nucleus and Mitochondria

Our analyses evinced extensive and intricate daily changes in the nuclear and mitochondrial lipidome under different feeding conditions and genetic backgrounds. Hence, in an attempt to identify broad organization principles, which might be suggestive of co-regulation of lipid species, we screened for lipids that show similar profiles throughout the various experimental conditions (i.e., wild-type fed ad libitum, night-fed wild-type, and PER1/2 null mice) in each organelle. First, we performed a pairwise correlation analysis for the lipid species in the nucleus and mitochondria and found a wide range of positively and negatively correlated lipids (Figure 7A). Positively correlating pairs were more abundant in the nucleus compared to mitochondria (median r value of 0.36 and 0.05 for the nucleus and mitochondria, respectively).

The positively correlated pairs spanned both intra- and inter-lipid classes and included also lipid pairs with different acyl-chain length and degree of saturation (Figure 7B). For example, the pairs LPE 18:1-LPE 20:4, LPE 18:2-PG 34:2, PC 34:1-PE

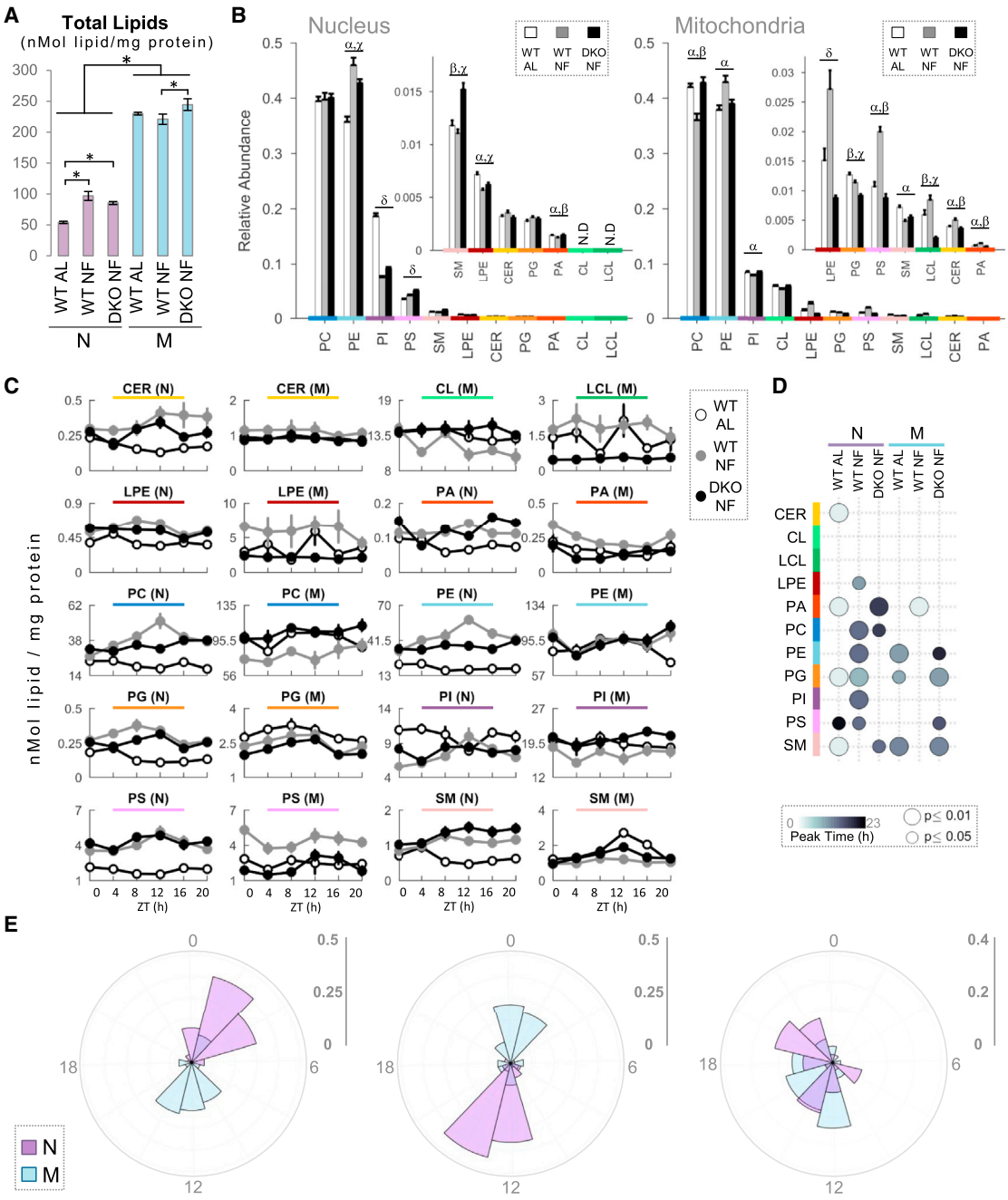

Figure 6. Comparison of the Nuclear and Mitochondrial Lipidome in Wild-Type and *Per1/2*$^{-/-}$ Mice under Different Feeding Regimens

(A) Comparison between the mean daily levels of the total lipids in the nucleus (N) and mitochondria (M) in wild-type mice fed ad libitum (WT AL), wild-type mice fed exclusively during the night (WT NF), and *Per1/2*$^{-/-}$ mice fed exclusively during the night (DKO NF). Data are presented as mean ± SD (six time points, n = 4 for each). Asterisks indicate significant change (FWER < 0.05).

(B) Comparison between the relative abundance of the different lipid classes in the nucleus and mitochondria of WT AL, WT NF, and DKO NF. Significant changes (FWER < 0.01) are indicated as follows: α, between WT AL and WT NF; β, between WT NF and DKO NF; χ, between WT AL and DKO NF; and δ, between all conditions in relation to each other. Data are presented as mean ± SEM.

(C) Comparison between the lipid abundance of the different lipid classes throughout the day in the nucleus and mitochondria of WT AL, WT NF, and DKO NF. Data are presented as mean ± SEM.

(D) Comparison of peak time (grayscale) and p value (point size) for the circadian lipid classes in each organelle/condition, based on JTK_CYCLE analysis (six time points, n = 4 for each; p < 0.05).

(E) A radar plot presentation of the peak phases of oscillating lipid species in the nucleus and mitochondria for WT AL, WT NF, and DKO NF. Data are corrected to the total number of oscillating lipid species in each condition.

See also Figures 3B, 4B, and 5B.

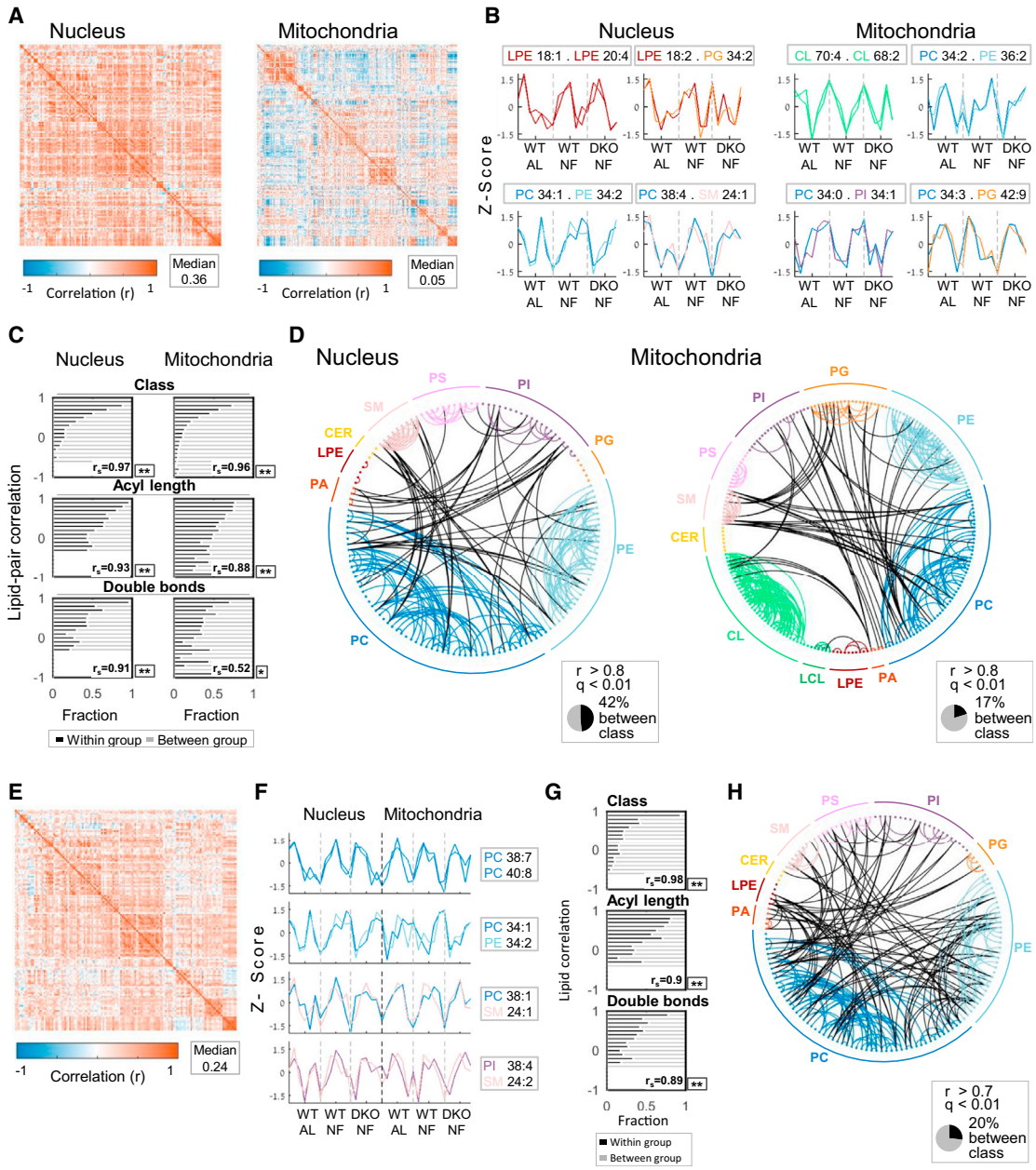

Figure 7. Network Analysis of the Nuclear and Mitochondrial Lipidome in Wild-Type and *Per1/2*$^{-/-}$ Mice under Different Feeding Regimens

(A) Correlation matrix sorted by lipid class. Rows and columns correspond to 146 lipid species measured in the nucleus (left) and 208 in mitochondria (right) across the different experimental setups (wild-type mice fed ad libitum and night-fed wild-type and *Per1/2*$^{-/-}$ mice). Color represents the correlation level between lipid pairs.

(B) Representative profiles of correlated lipids (r > 0.8), as measured in wild-type mice fed ad libitum (WT AL) and night fed (WT NF) and night-fed *Per1/2*$^{-/-}$ mice (DKO NF).

(C) Lipid pairs arranged based on correlation strength for the nucleus and mitochondria. The fraction of lipid pairs in each bin is grouped either between or within the same class, and similarity of fatty acid chain length (acyl length) or lipid saturation (double bonds) for lipids within the same class. r_s indicates positive trend by Spearman's rank correlation; *p < 0.05, **p < 0.01.

(D) Network visualization of correlated lipid pairs (r > 0.8) in the nucleus and mitochondria. Each lipid is represented by a node around the circle plot and color coded according to its class. Lines connecting highly correlated pairs are color coded according to lipid class for intra-class correlation, and are in black for inter-class correlation; 61 out of the 146 correlated pairs (42%) in the nucleus and 35 out of 208 correlated pairs (17%) in the mitochondria were between classes. FDR with q value <0.01.

(E) Correlation matrix sorted by class of 139 lipid species present both in the nucleus and mitochondria across the different experimental setups.

(F) Representative profiles of correlated lipids (r > 0.7), as measured in WT AL, WT NF, and DKO NF.

(G) Analysis as in (C) of lipids present both in the nucleus and mitochondria across the different experimental setups.

(H) Network visualization as in (D) of correlated lipid pairs (r > 0.7); 28 out of 139 correlated pairs (20%) were between classes. FDR with q value <0.01.

34:2, and PC 38:4-SM 24:1 exhibited a remarkable resemblance in their nuclear accumulation profiles under all tested conditions. Similarly, in mitochondria, CL 70:4-CL 68:2, PC 34:2-PE 36:2, PC 34:0-PI 34:1, and PC 34:3-PG 42:9 showed highly comparable profiles. This prompted us to examine potential parameters that might determine these correlations. Consistent with our observation that several lipid classes were relatively temporally homogeneous, we observed a higher correlation in lipid species within the same class (Figure 7C). In addition, we found that highly correlated lipids have similar acyl-chain length, whereas the saturation levels indicated by the number of carbon double bonds appeared to be less critical (Spearman's rank correlation). Along this line, some lipid classes were more disposed to correlate within themselves (e.g., PC in the nucleus and CL in mitochondria), whereas other families (e.g., LPE in the nucleus) exhibited more inter-class correlations (Figures 7D and S6A). Of note, SM in mitochondria showed both intra- and inter-class correlations. Overall, higher levels of inter-class relations were observed in the nucleus compared to mitochondria (42% and 17%, respectively).

Next, to attain a more global view of the intracellular lipid organization, we analyzed the pairwise correlation of lipid species present in the two organelles throughout the different experimental setups (i.e., 139 lipids) (Figure 7E). Remarkably, in this complex combination, we still detected highly correlated lipid pairs, for example PC 38:7-PC 40:8, PC 34:1-PE 34:2, PC 38:1-SM 24:2, and PI 38:4-SM 24:2 (Figure 7F). Positive correlations were more abundant within lipid families and similar acyl-chain length. The contribution of the number of double bonds was less prominent (Figure 7G). Specific analyses dedicated to fatty acid linkage (i.e., alkyl, diacyl, plasmalogen) in PC and PE revealed correlation between lipid species of the same linkage type (Figure S6B), with higher similarity in PC compared to PE classes. Collectively, we detected both intra- and inter-class similarities; for example, SM species showed high correlations within and between classes (Figures 7H and S6A).

In summary, our analyses shed light on potential predictive factors of inter- and intra-organelle lipid organization. These include lipid class and acyl-chain properties such as length, saturation, and linkage type.

DISCUSSION

Temporal and Spatial Lipidomics

In recent years, we have experienced significant advances in methodologies for lipid identification and quantification. However, we are still lacking comprehensive quantitative information regarding the lipid composition of intracellular organelles and their temporal dynamics. In this study, we performed extensive temporal and spatial lipid analyses. As a working model, we centered our efforts on two principal organelles, the nucleus and mitochondria. These two organelles largely differ in their cellular functions and morphology yet are defined by a distinct lipid bilayer, which comprises the bulk of lipids in both organelles.

Altogether, we collected quantitative information regarding the lipid content of the nucleus and mitochondria throughout the day in wild-type mice fed ad libitum and night-fed wild-type and clock-disrupted mice (i.e., PER1/2 null mice). Although technically, we are capable of identifying and quantifying hundreds of different lipid species, their specific functions are not fully known. Therefore, it is difficult to ascribe functional/physiological significance to the changes characterized in this study. However, we argue that our finding that similar lipid species are differentially temporally regulated is likely to reflect their specific functions. Hence, the comprehensive dataset presented in this study can serve as an important resource and lay the foundations for future studies on the lipids quantified herein.

Potential Functional Implications of Temporal Dynamics in Lipid Accumulation

Membrane lipids play an important role in membrane dynamics and organelle function. PC and PE are the two major constituents of lipid membranes, and their ratio is critical for membrane integrity (Li et al., 2006). We found that, although daily PC and PE levels were highly variable in the nucleus and mitochondria, under the different experimental setups, their ratio was consistently kept constant throughout the day. Thus, it appears that cells strictly maintain a constant daily PE/PC ratio in the different organelles, supporting the conception that their ratio is also critical for the integrity/function of organelles' membranes.

CL is an important component of the mitochondrial membrane and regulates the stability and activity of various membrane-bound protein complexes (e.g., respiratory complexes and the TIM/TOM protein import machinery) (Osman et al., 2011). Peek et al. (2013) were the first to report that mitochondrial fatty acid oxidation (FAO) is rhythmic. We recently corroborated their findings and identified diurnal oscillations in mitochondrial FAO in isolated mitochondria from mouse liver (Neufeld-Cohen et al., 2016). The zenith levels of FAO in wild-type mice at ~ZT4 correspond to the accumulation of specific CL species around the same time of the day. Remarkably, the majority of oscillating proteins in mitochondria accumulate in a daily manner with peak levels at ~ZT4, irrespective of their transcript levels (Neufeld-Cohen et al., 2016), suggesting that mitochondrial protein accumulation is primarily controlled through post-transcriptional mechanisms (e.g., mitochondrial protein translocation). The accumulation of CL at ~ZT4 and its role in the assembly/function of the TIM/TOM protein translocase complexes might support such a scenario.

Several studies have demonstrated that the mammalian nuclear receptors steroidogenic factor 1 (SF-1) and liver receptor homolog 1 (LRH-1) interact with PC, PE, and PG (Forman, 2005). Specifically, Li et al. (2005) further showed that phospholipids with C12–16 saturated fatty acyl groups can function as ligands for SF-1. Interestingly, we found that PC D16:0-16:0 accumulate at ~ZT0 in the nucleus of wild-type mice fed ad libitum and that nighttime-restricted feeding shifts its zenith levels to ~ZT14. It is possible that the rhythmic nuclear accumulation of PC D16:0-16:0 and its response to feeding might participate in the functional control of the above-mentioned nuclear receptors, in particular LRH-1, which plays an important role in lipid and cholesterol homeostasis.

CER serves as a signaling molecule in various cellular processes. It can be phosphorylated by ceramide kinase (CERK) to ceramide 1-phosphate (C1P) or utilized for the synthesis of

sphingomyelin. CER can also be broken down by ceramidases to sphingosine, which in turn is phosphorylated by sphingosine kinases to generate sphingosine 1-phosphate (S1P). Both C1P and S1P are considered important mediators of the inflammatory response by various mechanisms (Baumruker et al., 2005). Although we did not specifically detect C1P and S1P in our lipidomics analyses, we found that overall CER levels are oscillating exclusively in the nucleus, with CER N24:0, N24:1, and N24:2 reaching their zenith levels early in the light phase. It will be interesting to examine whether these specific nuclear CER species carry signaling functions or alternatively serve as a pool for C1P activity. By contrast, mitochondrial CER levels were relatively constant throughout the day, suggestive of their differential roles in the different organelles.

Lipids as Organelle Biomarkers

Whereas CL and LCL are widely considered hallmarks for mitochondrial lipids, a similar lipid marker for the nucleus is not well established (Osman et al., 2011). In line with previous reports, we identified CL and LCL in mitochondria. In addition, we detected several PG species, LPE P18:0, and CER N22:1 exclusively in mitochondria from all tested conditions (Figure S3H). Four lipid species were found throughout our entire analysis to be exclusively nuclear: PA 18:0-20:4, PE D18:0-18:0, PE P16:0-22:6, and PE P18:2-20:4 (Figure S3H). These lipids might potentially serve as unique biomarkers for the nucleus and mitochondria, yet currently we cannot exclude the possibility that these species are also present in other subcellular compartments that were not quantified in this study.

Lipids as a "Time Teller"

Previously, we reported that in mice fed ad libitum, 17% of quantified lipids in the liver exhibit circadian rhythmicity (Adamovich et al., 2014). In this study, we identified 34% and 31% oscillating lipids in the nucleus and mitochondria, respectively. The higher prevalence of cycling lipids in the different organelles compared to the whole organ can be readily explained by the dramatic phase differences between the two organelles. In the nucleus, most lipids peak at ZT2–4, whereas in mitochondria they reach their zenith levels at ZT12–14. This highlights the complexity in monitoring circadian rhythmicity, as whole-cell measurements mask oscillations within subcellular compartments. The current study together with our previous work on the whole-liver lipidome shows that lipids can also serve as a "time teller," and can be used to monitor circadian oscillations in organs and more specifically even in different intracellular organelles.

Historically, circadian time-measuring capacity in mammals was exclusively attributed to neurons in the suprachiasmatic nuclei in the brain. Similar oscillations were later recognized to be present in nearly every cell of the body (Schibler and Sassone-Corsi, 2002). Here, we add another layer of complexity and, by using lipids as a time teller, we uncover daily oscillations in subcellular compartments. The oscillations in the nucleus and mitochondria appear to be circadian clock controlled. At the molecular level, these rhythms might be systemically controlled or, even more excitingly, represent endogenous oscillations. Future studies with isolated organelles are expected to shed more light on the nature of these oscillations and reveal whether they are organelle autonomous and self-sustained.

The Effect of Time-Restricted Feeding on Lipid Composition of Intracellular Organelles

Several studies have demonstrated the metabolic benefits of time-restricted feeding (Asher and Sassone-Corsi, 2015). Nighttime-restricted feeding prevented obesity and metabolic syndrome in mice fed a high-fat diet (Chaix et al., 2014; Hatori et al., 2012). Furthermore, mice fed exclusively during the dark phase exhibited a dramatic decrease (~50%) in their hepatic triglyceride levels within 10 days (Adamovich et al., 2014). In this conjecture, we show that nighttime-restricted feeding also imposes substantial changes in the lipid composition of the nucleus and mitochondria. Moreover, in the nucleus, we observed a dramatic increase in lipid levels and the fraction of oscillating lipids. By contrast, in mitochondria, the lipid levels were unaltered and the fraction of cycling lipids dropped. Hence, it appears that the two organelles differentially respond to changes in feeding time. The concomitant effect of time-restricted feeding on both oscillation in gene expression and lipid cycling might support a cross-talk between the two processes.

Summary

The interest in the identification and characterization of myriad lipid species highlights the eminent importance of understanding principles in lipid organization. Recently, it was reported that proliferating cells actively regulate and modulate their lipid composition and localization during cell division (Atilla-Gokcumen et al., 2014). Furthermore, the cellular lipidome is widely described as undergoing changes as a consequence of different pathologies (Zhang and Wakelam, 2014) and can be used to predict the inflammatory response in patient-derived cells (Köberlin et al., 2015). These studies, together with our findings that there are daily oscillations in the lipid composition of intracellular organelles, are the first steps toward understanding the intricate regulation of cellular lipids.

In summary, we provide herein a comprehensive quantitative depiction of the nuclear and mitochondrial lipid landscape throughout the day and dissect their regulation by feeding time and the circadian clock.

EXPERIMENTAL PROCEDURES

Animals

All animal experiments and procedures were conducted in conformity with Institutional Animal Care and Use Committee (IACUC) guidelines. Three-month-old male wild-type and *Per1/2*$^{-/-}$ mice were used (Zheng et al., 2001). Mice were kept under a 12-hr light/dark regimen for 2 weeks and fed either ad libitum or exclusively during the dark phase. Mice were sacrificed at 4-hr intervals around the clock; livers were harvested and rinsed in PBS. ZT0 corresponded to the time lights were turned on and ZT12 to the time lights were turned off in the animal facility.

Nucleus and Mitochondria Isolation from Mouse Liver

Nuclei and mitochondria were isolated from mouse liver as previously described (Asher et al., 2010; Neufeld-Cohen et al., 2016) and detailed in the Supplemental Experimental Procedures.

Shotgun Lipidomics Analysis

Shotgun lipidomics analysis was performed as described (Han et al., 2012; Wang et al., 2016) and detailed in the Supplemental Experimental Procedures.

Lipidomics Data Analysis

Unless defined otherwise, p values are indicative of Student's t test, and data are shown as mean ± SEM. Normalized lipid values are defined as the lipid raw value for each ZT divided by the lipid daily mean value. Amplitude was defined as the ratio between the maximal and minimal values measured. Hierarchical clustering of the normalized lipidomics data was based on Euclidean distance with the "ward" center determination method, using the MATLAB linkage function (MathWorks). The number of clusters was selected by manual inspection of the distance matrices, and clusters consisting of five lipid species and fewer were excluded. Lipid class enrichment for each cluster was tested by random permutation of the species between the clusters for 10K iterations; the class enrichment threshold was set as family wise error rate (FWER) <0.025 for each organelle (Bonferroni correction). Intra-class variability (as in Figure S2B) was evaluated based on r^2 of each class cluster (i.e., variability = $1-(\sum_{i=1}^{n} r_i^2/n)$, wherein n is the number of lipid pairs within the class). We used Pearson correlations between the temporal profiles of lipid abundances to determine lipid-lipid correlations (Figures 2A, 2C, and 7). Analysis comparing lipids within different categories (Figures 7C, 7G, and S6B) was calculated as a function of correlation strength. Bins containing fewer than two lipid pairs were excluded. Analysis of length and saturation was applied to lipid pairs within the same class. Lipids with a delta of up to two carbons were considered to be within group for fatty acid chain length analysis. Likewise, lipids with up to one double-bond difference were considered to be within group for lipid saturation. Positive trend was evaluated by Spearman's rank correlation coefficient (r_s), and its p value was computed using random permutation of the category and its r values (10K iterations). Circular plots were created based on a modified circularGraph toolbox (MATLAB). The q value of Pearson's r was calculated by random permutation of each lipid abundance between time points for 10K iterations.

Kolmogorov-Smirnov test was used to compare between the distributions of pair-wise correlations (r values) of the different lipid species in Figure S2A. Lipid profiles were determined as "double peaks" using the findpeaks MATLAB function, with a threshold of >2.5 SEM minimum peak prominence.

Circadian Lipidomics Analysis

Rhythmicity of lipids was assessed with the nonparametric test JTK_CYCLE (Hughes et al., 2010). A window of 24 hr was used for the determination of circadian periodicity, and p value <0.05 was considered as statistically significant (corresponds to a false discovery rate [FDR] <0.17).

SUPPLEMENTAL INFORMATION

Supplemental Information includes Supplemental Experimental Procedures, six figures, and five tables and can be found with this article online at http://dx.doi.org/10.1016/j.molcel.2016.04.002.

AUTHOR CONTRIBUTIONS

G.A. and R.A. designed the experiments and wrote the paper. R.A., G.M., N.K., A.N.-C., Z.Z., M.E., Y.A., M.G., and C.W. conducted the experiments and analyzed the data. X.H. contributed analytic tools.

ACKNOWLEDGMENTS

We are grateful to S. Itzkovitz and all the members the G.A. laboratory for their advice and valuable comments on the manuscript. Work in the G.A. lab was supported by the Israel Science Foundation (ISF 138/12) and European Research Council (ERC-2011 METACYCLES 310320). G.A. is a recipient of the EMBO Young Investigator Award and incumbent of the Pauline Recanati Career Development Chair. Work in the X.H. lab was partly supported by National Institute of General Medical Sciences grant R01 GM105724, American Diabetes Association, and intramural institutional research funds.

Received: September 8, 2015
Revised: January 28, 2016
Accepted: April 1, 2016
Published: May 5, 2016

REFERENCES

Adamovich, Y., Rousso-Noori, L., Zwighaft, Z., Neufeld-Cohen, A., Golik, M., Kraut-Cohen, J., Wang, M., Han, X., and Asher, G. (2014). Circadian clocks and feeding time regulate the oscillations and levels of hepatic triglycerides. Cell Metab. *19*, 319–330.

Adamovich, Y., Aviram, R., and Asher, G. (2015). The emerging roles of lipids in circadian control. Biochim. Biophys. Acta *1851*, 1017–1025.

Andreyev, A.Y., Fahy, E., Guan, Z., Kelly, S., Li, X., McDonald, J.G., Milne, S., Myers, D., Park, H., Ryan, A., et al. (2010). Subcellular organelle lipidomics in TLR-4-activated macrophages. J. Lipid Res. *51*, 2785–2797.

Asher, G., and Sassone-Corsi, P. (2015). Time for food: the intimate interplay between nutrition, metabolism, and the circadian clock. Cell *161*, 84–92.

Asher, G., Reinke, H., Altmeyer, M., Gutierrez-Arcelus, M., Hottiger, M.O., and Schibler, U. (2010). Poly(ADP-ribose) polymerase 1 participates in the phase entrainment of circadian clocks to feeding. Cell *142*, 943–953.

Atilla-Gokcumen, G.E., Muro, E., Relat-Goberna, J., Sasse, S., Bedigian, A., Coughlin, M.L., Garcia-Manyes, S., and Eggert, U.S. (2014). Dividing cells regulate their lipid composition and localization. Cell *156*, 428–439.

Bass, J. (2012). Circadian topology of metabolism. Nature *491*, 348–356.

Baumruker, T., Bornancin, F., and Billich, A. (2005). The role of sphingosine and ceramide kinases in inflammatory responses. Immunol. Lett. *96*, 175–185.

Bird, S.S., Marur, V.R., Stavrovskaya, I.G., and Kristal, B.S. (2013). Qualitative characterization of the rat liver mitochondrial lipidome using LC-MS profiling and high energy collisional dissociation (HCD) all ion fragmentation. Metabolomics *9* (1 Suppl), 67–83.

Brügger, B. (2014). Lipidomics: analysis of the lipid composition of cells and subcellular organelles by electrospray ionization mass spectrometry. Annu. Rev. Biochem. *83*, 79–98.

Chaix, A., Zarrinpar, A., Miu, P., and Panda, S. (2014). Time-restricted feeding is a preventative and therapeutic intervention against diverse nutritional challenges. Cell Metab. *20*, 991–1005.

Damiola, F., Le Minh, N., Preitner, N., Kornmann, B., Fleury-Olela, F., and Schibler, U. (2000). Restricted feeding uncouples circadian oscillators in peripheral tissues from the central pacemaker in the suprachiasmatic nucleus. Genes Dev. *14*, 2950–2961.

Feng, D., and Lazar, M.A. (2012). Clocks, metabolism, and the epigenome. Mol. Cell *47*, 158–167.

Forman, B.M. (2005). Are those phospholipids in your pocket? Cell Metab. *1*, 153–155.

Han, X., Yang, K., and Gross, R.W. (2012). Multi-dimensional mass spectrometry-based shotgun lipidomics and novel strategies for lipidomic analyses. Mass Spectrom. Rev. *31*, 134–178.

Hatori, M., Vollmers, C., Zarrinpar, A., DiTacchio, L., Bushong, E.A., Gill, S., Leblanc, M., Chaix, A., Joens, M., Fitzpatrick, J.A., et al. (2012). Time-restricted feeding without reducing caloric intake prevents metabolic diseases in mice fed a high-fat diet. Cell Metab. *15*, 848–860.

Hughes, M.E., Hogenesch, J.B., and Kornacker, K. (2010). JTK_CYCLE: an efficient nonparametric algorithm for detecting rhythmic components in genome-scale data sets. J. Biol. Rhythms *25*, 372–380.

Klose, C., Surma, M.A., and Simons, K. (2013). Organellar lipidomics—background and perspectives. Curr. Opin. Cell Biol. *25*, 406–413.

Köberlin, M.S., Snijder, B., Heinz, L.X., Baumann, C.L., Fauster, A., Vladimer, G.I., Gavin, A.C., and Superti-Furga, G. (2015). A conserved circular network of coregulated lipids modulates innate immune responses. Cell *162*, 170–183.

Li, Y., Choi, M., Cavey, G., Daugherty, J., Suino, K., Kovach, A., Bingham, N.C., Kliewer, S.A., and Xu, H.E. (2005). Crystallographic identification and functional

characterization of phospholipids as ligands for the orphan nuclear receptor steroidogenic factor-1. Mol. Cell *17*, 491–502.

Li, Z., Agellon, L.B., Allen, T.M., Umeda, M., Jewell, L., Mason, A., and Vance, D.E. (2006). The ratio of phosphatidylcholine to phosphatidylethanolamine influences membrane integrity and steatohepatitis. Cell Metab. *3*, 321–331.

Liu, S., Brown, J.D., Stanya, K.J., Homan, E., Leidl, M., Inouye, K., Bhargava, P., Gangl, M.R., Dai, L., Hatano, B., et al. (2013). A diurnal serum lipid integrates hepatic lipogenesis and peripheral fatty acid use. Nature *502*, 550–554.

Neufeld-Cohen, A., Robles, M.S., Aviram, R., Manella, G., Adamovich, Y., Ladeuix, B., Nir, D., Rousso-Noori, L., Kuperman, Y., Golik, M., et al. (2016). Circadian control of oscillations in mitochondrial rate-limiting enzymes and nutrient utilization by PERIOD proteins. Proc. Natl. Acad. Sci. USA *113*, E1673–E1682.

Osman, C., Voelker, D.R., and Langer, T. (2011). Making heads or tails of phospholipids in mitochondria. J. Cell Biol. *192*, 7–16.

Partch, C.L., Green, C.B., and Takahashi, J.S. (2014). Molecular architecture of the mammalian circadian clock. Trends Cell Biol. *24*, 90–99.

Peek, C.B., Affinati, A.H., Ramsey, K.M., Kuo, H.Y., Yu, W., Sena, L.A., Ilkayeva, O., Marcheva, B., Kobayashi, Y., Omura, C., et al. (2013). Circadian clock NAD^+ cycle drives mitochondrial oxidative metabolism in mice. Science *342*, 1243417.

Schibler, U., and Sassone-Corsi, P. (2002). A web of circadian pacemakers. Cell *111*, 919–922.

Shevchenko, A., and Simons, K. (2010). Lipidomics: coming to grips with lipid diversity. Nat. Rev. Mol. Cell Biol. *11*, 593–598.

van Meer, G., Voelker, D.R., and Feigenson, G.W. (2008). Membrane lipids: where they are and how they behave. Nat. Rev. Mol. Cell Biol. *9*, 112–124.

Vollmers, C., Gill, S., DiTacchio, L., Pulivarthy, S.R., Le, H.D., and Panda, S. (2009). Time of feeding and the intrinsic circadian clock drive rhythms in hepatic gene expression. Proc. Natl. Acad. Sci. USA *106*, 21453–21458.

Wang, M., Wang, C., Han, R.H., and Han, X. (2016). Novel advances in shotgun lipidomics for biology and medicine. Prog. Lipid Res. *61*, 83–108.

Zhang, Q., and Wakelam, M.J. (2014). Lipidomics in the analysis of malignancy. Adv. Biol. Regul. *54*, 93–98.

Zheng, B., Albrecht, U., Kaasik, K., Sage, M., Lu, W., Vaishnav, S., Li, Q., Sun, Z.S., Eichele, G., Bradley, A., and Lee, C.C. (2001). Nonredundant roles of the mPer1 and mPer2 genes in the mammalian circadian clock. Cell *105*, 683–694.